Analysis of hippocampal gene expression profile of Alzheimer's disease model rats using genome chip bioinformatics☆

Yinghong Li[1], Zhengzhi Wu[1, 2], Yu Jin[1], Anmin Wu[1], Meiqun Cao[2], Kehuan Sun[1], Xiuqin Jia[1], Manyin Chen[1]

1 *First Affiliated Hospital of Shenzhen University/Second People's Hospital of Shenzhen City, Shenzhen 518035, Guangdong Province, China*
2 *Second Clinical Medical College of Jinan University/Shenzhen Institute of Geriatrics, Shenzhen 518020, Guangdong Province, China*

Abstract

In this study, an Alzheimer's disease model was established in rats through stereotactic injection of condensed amyloid beta 1–40 into the bilateral hippocampus, and the changes of gene expression profile in the hippocampus of rat models and sham-operated rats were compared by genome expression profiling analysis. Results showed that the expression of 50 genes was significantly up-regulated (fold change ≥ 2), while 21 genes were significantly down-regulated in the hippocampus of Alzheimer's disease model rats (fold change ≤ 0.5) compared with the sham-operation group. The differentially expressed genes are involved in many functions, such as brain nerve system development, neuronal differentiation and functional regulation, cellular growth, differentiation and apoptosis, synaptogenesis and plasticity, inflammatory and immune responses, ion channels/transporters, signal transduction, cell material/energy metabolism. Our findings indicate that several genes were abnormally expressed in the metabolic and signal transduction pathways in the hippocampus of amyloid beta 1–40-induced rat model of Alzheimer's disease, thereby affecting the hippocampal and brain functions.
Key Words: amyloid beta 1–40; Alzheimer's disease; hippocampus; genome chip; gene expression profile; neural regeneration

INTRODUCTION

Alzheimer's disease (AD), also known as presenile dementia or senile dementia, is a type of central nervous system degenerative disease characterized by progressive cognitive impairment and memory damage. It is the most common type of dementia[1-2]. AD has three major pathological features: senile plaque formation as a result of amyloid beta (Aβ) accumulation around brain cells, neurofibrillary tangle formation as a result of Tau protein hyperphosphorylation within brain cells, and neuronal death. Aβ peptide accumulation is a crucial factor leading to AD, and is one of the neuropathological markers of AD[3-4]. However, the occurrence and development of AD is a complex pathological process involving many factors and pathways, where many genes play a synergistic (or antagonistic) role. This process includes the shearing, hydrolysis and clearing of amyloid protein precursor; imbalance of protein phosphorylation, neuronal apoptosis, DNA transcription, protein synthesis, signal transduction, and other changes of related genes[5-6]. It remains unknown which genes

are involved in AD occurrence and development, and impedes attempts to explore the prevention and treatment of AD. Gene chip, a recently developed technology, has been widely applied in understanding gene functions, investigating the links between genes, analyzing spatial and temporal expression of each gene[7-12], and exploring the downstream signal transduction pathways[13-14]. It is a high throughput technology that is fast and requires only small amounts of samples, but yields copious information. With the application of gene chip and in-depth study of central nervous system regeneration, we have achieved great progress in the research of central nervous system diseases. Gene chip technology has been recognized as a powerful means for studying the mechanism underlying the multi-gene, multi-pathway, multi-factorial components of neurological diseases, and for elucidating the correlation of genes to neurological diseases. The present study sought to understand and diagnose central nervous system diseases, as well as to identify potential genetic therapy and drug treatment.

The hippocampus is an important brain

region for neurogenesis in the adult brain, and participates in the formation of learning and memory, and the regulation of mood. A number of studies have shown that the learning and memory functions are significantly decreased in a damaged bilateral hippocampus, thus affecting learning, maintenance of defense conditioned response, and spatial acquisition capabilities[15-16]. Intraventricular injection of toxic Aβ fragments can lead to a decrease in learning and memory in animals, and can partially simulate the pathological hallmarks of AD[17]. In this study, AD rat models were established through $A\beta_{1-40}$ injection into the bilateral hippocampus of rats. The microarray expression profiling changes in the hippocampus of AD rats were determined with whole genome microarray analysis, and the AD-associated genes and gene expression profiles were observed in a broader attempt to elucidate the etiology of AD at the gene level, to identify the molecular genetic mechanisms underlying the $A\beta_{1-40}$-induced AD, to search drug targets for the prevention and treatment of AD, and to provide laboratory evidence for screening effective drugs for the prevention and treatment of AD.

RESULTS

Quantitative analysis of experimental animals

Thirty male Sprague-Dawley rats, of specific pathogen-free grade, were maintained for 2 weeks for acclimation, and 22 of the animals that were in good condition were used in further study. A total of 22 rats were divided into a sham-operation group ($n = 10$) and an AD model group ($n = 12$) according to a random number table. Normal saline and $A\beta_{1-40}$ was injected into the bilateral hippocampi, respectively. Eight rats were confirmed for AD-like behaviors by use of Morris water maze test at 4 weeks post-surgery. Finally, five rats were randomly selected from two groups for whole-genome microarray analysis of the hippocampus.

Identification of RNA in the hippocampus of $A\beta_{1-40}$-induced AD model rats and sham-operated rats

Total RNA was extracted from the hippocampus of each group by using RNAEx Reagent, and quantified with a UV spectrophotometer. The ratio of absorbance at 260 nm and 280 nm was 1.8–2.0, indicating a high purity of RNA. Formaldehyde denaturing gel electrophoresis detection showed that the electrophoresis strip of RNA samples was clear and the luminance ratio of the rRNA band at 28 S to 18 S was greater than 1: 1, indicating that RNA was intact and met the requirements for expression profiling microarray and the reverse transcription-PCR test (Figure 1).

Changes of gene expression in rat hippocampus after $A\beta_{1-40}$ treatment

In this study, gene expression profile was examined with whole genome microarray analysis (Figure 2). As shown in the microarray hybridization signal intensity plot, the vast majority of hybridization signals were located

around the 45° diagonal line. The ratio of Y value and X value was 0.5–2.0, indicating non-differential expression; the minor number of data points were substantially away from the 45° diagonal line. The ratio of Y value and X value was out of the range between 0.5 and 2.0, indicating differential expression (Figure 3).
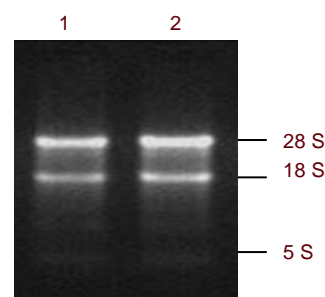

Figure 1 RNA was extracted from the rat hippocampus with 1% formaldehyde denaturing gel electrophoresis. Image was provided by the National Engineering Research Center for Beijing Biochip Technology (Beijing CapitalBio Corporation, China).

The RNA sample electrophoretic bands were clear. rRNA band intensity at 28 S to 18 S was larger than 1: 1, in accordance with the quality requirements of microarray experiments. The RNA integrity was good with fewer degraded small fragments.

1: Sham-operation group; 2: Alzheimer's disease model group.
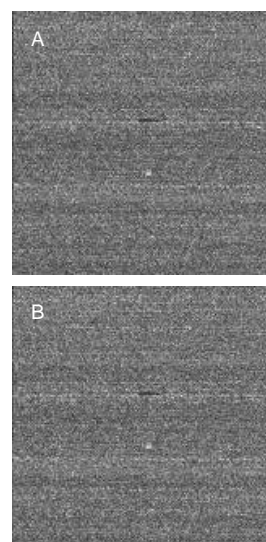
Figure 2 Original image of hippocampal gene expression profile. Image was provided by the National Engineering Research Center for Beijing Biochip Technology (Beijing CapitalBio Corporation, China) who provided the original microarray data plot for the DNA microarray experiments of the samples in two groups.

(A) Sham-operation group; (B) Alzheimer's disease model group.

Comparison of gene expression changes in the hippocampus of each group showed that the expressions of fifty genes in the hippocampus of the model group

were significantly up-regulated (fold change ≥ 2), while the expressions were down-regulated in 21 genes (fold change ≤ 0.5) compared with the sham-operation group. Gene biological functions were evaluated with MAS software, and results showed that the vast majority of differentially expressed genes were associated with the immune response, and many up-regulated genes and cell cycle-related protein factors were seen. A variety of transcription-related genes were also up-regulated, due to activation of the transcription control system, and up-regulation of the genes involved in the intracellular signal transduction pathway. Furthermore, many cytokines and their receptors, intracellular enzyme- or protein-related genes were up-regulated, and the most significant difference was observed in LOC500180 (FC = 22.5), IgH-1a (FC = 12.7), and LOC4983359 (FC = 11) which all participate in the immune response (Table 1).

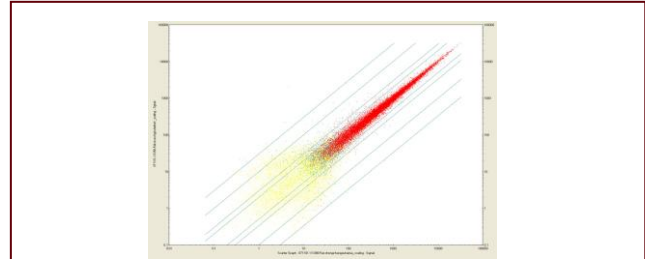Figure 3   Scatter plot of gene hybridization signal intensity in two groups. Image was provided by the National Engineering Research Center for Beijing Biochip Technology (Beijing CapitalBio Corporation, China), through a paired comparison of the original microarray data in the sample analysis process.

Vertical axis represents the scaling signal (intensity) in the Alzheimer's disease model group, while the X-axis represents the scaling signal (intensity) in the sham-operation group.

Table 1   Differentially expressed genes in the hippocampus of amyloid beta 1−40-injected Alzheimer's disease model rats compared with sham-operated rats (*n* = 5)

Gene	Fold change (mean ± SD)	Biological process or pathway
LOC500180	22.50±1.61	Antigen binding // immune response
Igh-1a	12.70±1.13	Antibody-dependent cellular cytotoxicity // positive regulation of type I or iia hypersensitivity // phagocytosis, recognition // engulfment // complement activation, classical pathway // endosome to lysosome transport // immunoglobulin mediated immune response // antigen processing and presentation // regulation of proteolysis // early endosome to late endosome transport // positive regulation of endocytosis // positive regulation of phagocytosis // positive regulation of immune response // positive regulation of B cell activation
LOC4983359	11.00±1.28	Immune response
LOC689064	9.46±1.15	Transport // oxygen transport // protein hetero-oligomerization
Msr2	5.91±0.37	Scavenger receptor activity
IgG-2a	5.71±0.20	Cell redox homeostasis
Coch	4.83±0.29	Sensory perception of sound
Col3a1	4.81±0.41	Inflammatory response pathway // skeletal development // phosphate transport // blood circulation // organ morphogenesis
RT1-CE5	4.53±0.51	Induction of apoptosis // positive regulation of neuron apoptosis // inflammatory response // immune response // signal transduction // negative regulation of cell proliferation //cell activation // negative regulation of L-glutamate transport // antigen processing and presentation of peptide antigen *via* MHC class I // response to mechanical stimulus // calcium-mediated signaling // antigen processing and presentation // macrophage activation // positive regulation of I-kappab kinase/NF-kappab cascade // positive regulation of mitosis // negative regulation of glucose import // positive regulation of synaptic transmission // positive regulation of protein transport
Tnnt1	4.30±0.37	Regulation of muscle contraction // slow-twitch skeletal muscle fiber contraction // striated muscle contraction
Col1a2	4.26±0.21	Skeletal development //phosphate transport // transmembrane receptor protein tyrosine kinase signaling pathway // inflammatory response pathway
Scn7a	3.98±0.40	Ion transport // cation transport // sodium ion transport // calcium ion transport
Cxcl4	3.96±0.27	Chemotaxis // immune response // negative regulation of angiogenesis // cytokine and chemokine mediated signaling pathway //platelet activation // leukocyte chemotaxis // negative regulation of megakaryocyte differentiation
Obp3	3.57±0.26	Transport
RT1-Ba	3.56±0.41	Inflammatory response pathway // antigen processing and presentation of peptide or polysaccharide antigen *via* MHC class II // immune response // antigen processing and presentation // peptide antigen transport
Lcat	3.54±0.29	Statin Pathway pharmgkb // lipid metabolic process // steroid metabolic process // cholesterol metabolic process // cholesterol metabolic process // protein amino acid esterification // lipoprotein metabolic process // lipoprotein biosynthetic process // response to copper ion // response to glucocorticoid stimulus
Dusp1	3.45±0.30	Protein amino acid dephosphorylation // response to oxidative stress // cell cycle // intracellular signaling cascade // dephosphorylation
Gpr88	3.44±0.33	Signal transduction // G-protein coupled receptor protein signaling pathway
Nupr1	3.24±0.25	Cell growth
Fos	3.09±0.22	DNA methylation // regulation of transcription, DNA-dependent // regulation of transcription from RNA polymerase II promoter // inflammatory response // nervous system development
C7/Tubb2c	3.05±0.18	Induction of apoptosis // microtubule-based process // microtubule-based movement // protein polymerization // cellular sodium ion homeostasis
RT1-Da	2.90±0.23	Antigen processing and presentation of peptide or polysaccharide antigen *via* MHC class II // immune response // peptide antigen transport

Table 1 Continued

Gene	Fold change (mean ± SD)	Biological process or pathway
Nfkbia	2.82±0.21	Apoptosis // protein import into nucleus, translocation // cytoplasmic sequestering of NF-kappaB // response to bacterium // lipopolysaccharide-mediated signaling pathway // response to lipopolysaccharide // regulation of cell proliferation // regulation of NF-kappaB import into nucleus // response to exogenous dsRNA // negative regulation of DNA binding // negative regulation of myeloid cell differentiation // negative regulation of myeloid cell differentiation // negative regulation of Notch signaling pathway
Cldn1	2.81±0.19	Cell adhesion // calcium-independent cell-cell adhesion // myelination
Serping1	2.75±0.16	Immune response // complement activation, classical pathway // blood coagulation
Aldh1a2	2.75±0.24	Neural crest cell development // morphogenesis of embryonic epithelium // neuron differentiation // embryonic limb morphogenesis // forebrain // hindbrain development // heart morphogenesis // vitamin A metabolic process // positive regulation of cell proliferation // determination of bilateral symmetry // proximal/distal /anterior/posterior pattern formation // pancreas development // retinoic acid metabolic process // camera-type eye development // retinoic acid receptor signaling pathway
Cxcl10	2.74±0.28	Electron transport // cell motility // chemotaxis // inflammatory response // immune response // signal transduction // muscle development // positive regulation of cell proliferation or migration // protein secretion
Arf4l	2.74±0.14	Intracellular protein transport // protein secretion // vesicle-mediated transport
Cd74	2.68±0.11	Immunoglobulin mediated immune response // activation of MAPK activity // prostaglandin biosynthetic process // protein complex assembly // intracellular protein transport // defense response // antigen processing and presentation of exogenous peptide antigen *via* MHC class II // negative regulation of apoptosis // thymic T cell selection // regulation of T cell differentiation // chaperone cofactor-dependent protein folding // cell proliferation
Egr2	2.63±0.14	Brain development // peripheral nervous system development // learning and/or memory // rhythmic behavior // Schwann cell differentiation // hindbrain development // response to insulin stimulus // myelination // regulation of neuronal synaptic plasticity // transcription // regulation of transcription, DNA-dependent
Cybb	2.62±0.15	Electron transport // response to nutrient // response to drug
C4-2/C4a	2.60±0.20	I-kappab kinase // NF-kappab cascade // JAK-STAT cascade // nervous system development // brain development // aging // positive regulation of Wnt receptor signaling pathway // defense response // inflammatory response // immune response // complement activation classical pathway // response to unfolded protein // innate immune response // positive regulation of smooth muscle contraction // response to nutrient // immunoglobulin mediated immune response // glucocorticoid mineralocor-ticoid metabolism
RT1-N1/N2/N3	2.55±0.21	Antigen processing and presentation of peptide antigen *via* MHC class I // immune response
Fxyd6	2.52±0.27	Transport // ion transport
Plekhh1	2.39±0.15	Motor activity // actin binding // ATP binding
Cpxm2	2.27±0.12	Proteolysis // cell adhesion
Fmo1	2.26±0.10	Transport // electron transport
Sgk	2.22±0.20	Protein amino acid phosphorylation // sodium ion transport // cellular sodium ion homeostasis // apoptosis // response to stress // response to DNA damage stimulus // cell communication
Plekhf1	2.19±0.18	Induction of apoptosis
Gpnmb	2.18±0.31	Osteoblast differentiation // cell adhesion // metabolic process // negative regulation of cell proliferation // bone mineralization
Klf2	2.17±0.16	Transcription // regulation of transcription, DNA-dependent // positive regulation of transcription
Camk2d	2.14±0.28	G_1/S transition of mitotic cell cycle // regulation of cell growth // response to hypoxia // protein amino acid phosphorylation // protein amino acid phosphorylation // calcium ion transport // cellular potassium ion homeostasis // protein amino acid autophosphorylation // calcium regulation in cardiac cells // smooth muscle contraction
Rbm3	2.13±0.15	GTP/UTP/CTP biosynthetic process // RNA processing // response to cold // mirna-mediated gene silencing, production of mirnas
Prkcd	2.03±0.26	Induction of apoptosis // Wnt signaling // intracellular signaling cascade // G protein signaling // immunoglobulin mediated immune response // interleukin-10 production // interleukin-12 production // B cell proliferation // calcium regulation in cardiac cells // protein amino acid phosphorylation // smooth muscle contraction
Zfp54	2.02±0.17	Regulation of transcription, DNA-dependent
Elk4	2.02±0.19	Transcription from RNA polymerase II promoter
Snf1lk	2.02±0.11	Negative regulation of transcription from RNA polymerase II promoter // protein amino acid phosphorylation // cell cycle // protein kinase cascade //multicellular organismal development // regulation of mitotic cell cycle // cell differentiation //regulation of cell differentiation
Rgs1	2.01±0.14	Immune response //signal transduction // G-protein coupled receptor protein signaling pathway // G-protein signaling, adenylate cyclase inhibiting pathway // negative regulation of signal transduction // calcium regulation in cardiac cells // smooth muscle contraction
LOC688090	2.01±0.11	Antigen processing and presentation of peptide or polysaccharide antigen *via* MHC class II // immune response // peptide antigen transport
Ddit4	2.00±0.16	Apoptosis // negative regulation of signal transduction // response to hypoxia
Ttr	0.06±0.02	Thyroid hormone generation // transport // thyroid hormone metabolic process
Camkk2	0.22±0.05	Protein amino acid phosphorylation
RGD1564056	0.23±0.04	tRNA aminoacylation for protein translation
Gabbr1	0.28±0.05	Gamma-aminobutyric acid signaling pathway//negative regulation of adenylate cyclase activity // GPCRDB Class A Rhodopsin-like // GPCRDB Class C Metabotropic glutamate pheromone // osteoblast differentiation // signal transduction // G-protein coupled receptor protein signaling pathway

Table 1   Continued

Gene	Fold change (mean ± SD)	Biological process or pathway
Comt	0.28±0.03	Catecholamine metabolic process // neurotransmitter catabolic process // dopamine metabolic process // dopamine catabolic process // S-adenosylhomocysteine metabolic process // biogenic amine synthesis
Sostdc1	0.31±0.02	Wnt receptor signaling pathway // negative regulation of BMP signaling pathway // pattern specification process // embryo implantation // odontogenesis of dentine-containing teeth
Cd3e	0.32±0.03	Response to nutrient // positive regulation of T cell proliferation // T cell activation // regulation of apoptosis // negative thymic T cell selection // lymphocyte activation //positive regulation of peptidyl-tyrosine phosphorylation // positive regulation of calcium-mediated signaling // T cell receptor signaling pathway
Fkhl18	0.35±0.04	Transcription // regulation of transcription, DNA-dependent // multicellular organismal development
Rabl4	0.36±0.02	Small GTPase mediated signal transduction
Jund	0.42±0.05	Regulation of transcription, DNA-dependent // regulation of transcription from RNA polymerase II promoter
Atxn1	0.42±0.05	Brain morphogenesis // adult locomotory behavior // visual learning // negative regulation of transcription // nuclear export // regulation of excitatory postsynaptic membrane potential
Homer1	0.45±0.04	Synaptic transmission // metabotropic glutamate receptor, phospholipase C activating pathway // metabotropic glutamate receptor signaling pathway
Pldn	0.46±0.06	Vesicle docking during exocytosis // vesicle fusion // membrane fusion // synaptic vesicle docking during exocytosis
Kcnc2	0.46±0.04	Transport // ion transport // cation transport // potassium ion transport
Clec14a	0.46±0.05	Proteolysis
LOC682058	0.46±0.04	RNA metabolic process
Taf7l	0.47±0.06	Regulation of transcription
Txnl1	0.49±0.05	Electron transport // transport // apoptosis // signal transduction // regulation of cell redox homeostasis // cell redox homeostasis
Gabrb2	0.49±0.06	Transport // ion transport // gamma-aminobutyric acid signaling pathway // synaptic transmission
Ddit4l	0.50±0.05	Negative regulation of signal transduction
Tnfrsf11b	0.50±0.07	Apoptosis // signal transduction // response to nutrient // response to inorganic substance // response to magnesium ion // negative regulation of odontogenesis of dentine-containing teeth // response to drug // response to estrogen stimulus // negative regulation of osteoclast differentiation // negative regulation of bone resorption // response to arsenic // skeletal development

FC: Fold change value of $A\beta_{1-40}$-induced Alzheimer's disease model and sham-operated rats; FC ≥ 2: gene expression was differentially up-regulated; FC ≤ 0.5: gene expression was differentially down-regulated.

LOC: Locus; Igh-1a: immunoglobulin heavy chain 1a; Msr2: Fc receptor-like S, scavenger receptor; IgG-2a: gamma-2a immunoglobulin heavy chain; COCH: coagulation factor C homolog, cochlin; Col3a1: collagen, type III, alpha 1; RT1-CE5: RT1 class I, locus CE5; Tnnt1: troponin T type 1; Col1a2: collagen, type I, alpha 2; Scn7a: sodium channel, voltage-gated, type VII, alpha; Cxcl4: platelet factor 4; Obp3: odorant binding protein 3; RT1-Ba: RT1 class II, locus Ba; Lcat: lecithin-cholesterol acyltransferase; Dusp1: dual specificity phosphatase 1.

Gpr88: G-protein coupled receptor 88; Nupr1: Nupr1nuclear protein 1; Fos: FBJ murine osteosarcoma viral oncogene homolog; C7: complement component 7; Tubb2c: tubulin, beta 2C; RT1-Da: RT1 class II, locus Da; Nfkbia: nuclear factor of kappa light polypeptide gene enhancer in B-cells inhibitor, alpha; Cldn1: claudin 1; Serping1: serpin peptidase inhibitor, clade G (C1 inhibitor), member 1; Aldh1a2: aldehyde dehydrogenase 1 family, member A2; Cxcl10: chemokine (C-X-C motif) ligand 10; Arf4l: ADP-ribosylation factor-like 4D.

Cd74: CD74 molecule, major histocompatibility complex, class II invariant chain; Egr2: early growth response 2; Cybb: cytochrome b-245, beta polypeptide; C4-2: complement component 4, gene 2; C4a: complement component 4A (Rodgers blood group); RT1-N1: RT1 class Ib, locus N1; Fxyd6: FXYD domain containing ion transport regulator 6; Plekhh1: pleckstrin homology domain containing, family H (with MyTH4 domain) member 1; Cpxm2: carboxypeptidase X (M14 family), member 2; Fmo1: flavin containing monooxygenase 1.

Sgk: Serum/glucocorticoid regulated kinase; Plekhf1: pleckstrin homology domain containing, family F (with FYVE domain) member 1; Gpnmb: glycoprotein (transmembrane) nmb; Klf2: Kruppel-like factor 2; Camk2d: calcium/calmodulin-dependent protein kinase II delta; Rbm3: RNA binding motif (RNP1, RRM) protein 3; Prkcd: protein kinase C, delta; Zfp54: zinc finger protein 54; Elk4: ETS-domain protein (SRF accessory protein 1); Snf1lk: SNF1-like kinase; Rgs1: regulator of G-protein signaling 1; Ddit4: DNA-damage-inducible transcript 4.

Ttr: Transthyretin; Camkk2: calcium/calmodulin-dependent protein kinase kinase 2; Gabbr1: gamma-aminobutyric acid (GABA) B receptor, 1; Comt: catechol-O-methyltransferase; Sostdc1: sclerostin domain containing 1; Cd3e: CD3e molecule, epsilon (CD3-TCR complex) ; Fkhl18: forkhead-like 18; Rabl4: RAB, member of RAS oncogene family-like 4; Jund: jun D proto-oncogene; Atxn1: ataxin 1; Homer1: homer homolog 1; Pldn: pallidin homolog; Kcnc2: potassium voltage-gated channel, Shaw-related subfamily, member 2.

Clec14a: C-type lectin domain family 14, member A; Taf7l: TAF7-like RNA polymerase II, TATA box binding protein (TBP)-associated factor; Txnl1: thioredoxin-like 1; Gabrb2: gamma-aminobutyric acid (GABA) A receptor, beta 2; Ddit4l: DNA-damage-inducible transcript 4-like; Tnfrsf11b: tumor necrosis factor receptor superfamily, member 11b.

DISCUSSION

The recently developed gene chip technology can detect the expression of thousands of genes simultaneously, and can form a complete gene expression profile. It has become a powerful tool for the analysis of gene expression. Gene microarray can simultaneously detect the mRNA expression of different genes in varying tissues or cells at different developmental stages within the entire genome[7-12], therefore, it is an ideal approach for studying the pathological mechanisms underlying AD. In this study, the pathological process of AD animals was simulated through injection of $A\beta_{1-40}$ into the bilateral

hippocampus. The hippocampal gene expression profile changes were compared between the sham-operated group and the AD model group with the whole genome microarray analysis. Results showed that the expressions were significantly up-regulated in 50 genes in the hippocampus of the model group (fold change ≥ 2), while significantly down-regulated in 21 genes (fold change ≤ 0.5) compared with the sham-operation group. The up-regulated genes in the $A\beta_{1-40}$-induced AD rats, such as nuclear factor of kappa light polypeptide gene enhancer in B-cells inhibitor (α-Nfkbia) (FC = 2.82), can bind with nuclear factor κB and regulate its intracellular degradation, participate in lipopolysaccharide-mediated signaling pathways and inflammatory responses, inhibit the differentiation of bone marrow stem cells and DNA binding, and reversibly control the Notch signaling pathway. The Notch signaling pathway, activated by ligand binding, can switch the conversion of the cell cycle, regulate cell apoptosis and fate, affect the nervous system formation and morphogenesis, and contribute to the differentiation and development of the nervous system[18-23].

Notch signaling is not independent of the Wnt signaling pathway, as these two signaling pathways can crosstalk through Dsh. Dsh is activated by Wnt signaling and plays an antagonistic role against Notch signaling. The Wnt gene is a highly conserved family, which is involved in the body axis and germ layer formation, organogenesis and development, stem cell differentiation and cell fate in normal embryonic development. A number of studies have shown that the Wnt signaling pathway is the key pathway for the regulation of cell growth and proliferation of the vertebrate central nervous system, and especially the development of hippocampal and cortical 2/3 neurons. During embryonic nervous system development, the Wnt signaling pathway determines the spatial and temporal proliferation and differentiation of neural stem cells[24-27]. Thus, the Wnt signaling pathway has received close attention in studies regarding nervous system diseases.

The cerebral cortex, hippocampus, and entorhinal cortex, which are associated with learning, memory, and other senior functions, are the most vulnerable sites in the AD pathological process. Presenilin, Notch, and Wnt are highly expressed in these brain regions. However, Notch and Wnt signaling system disorders in neuronal plasticity may lead to neural degeneration diseases. Recent studies have shown that changes in several signaling molecules in the Wnt signaling pathway are related to the formation of Aβ and the development of AD[28-29].

Lecithin cholesterol acyltransferase (FC = 3.54) is involved in lipid metabolism, and may be related to cell lipid metabolism in the nervous system. Lecithin cholesterol acyltransferase contributes to steroid and lipid metabolism, and statin signal transduction pathways, and regulates Aβ formation and brain functions[30-32].

Protein kinase Cδ (FC = 2.03) is a substrate of caspase-3 and induces cellular apoptosis, and is responsible for the regulation of Wnt and G protein signal transduction pathways, while the interleukin-10/12 mediate the immune response.

The down-regulated gene in the $A\beta_{1-40}$-induced AD model group, γ-aminobutyric acid (GABA) B receptor 1 subunit (FC = 0.277), can control the γ-GABA and G-protein receptor signaling pathways, and inhibit glandular nucleotide cyclase activity. GABA is an important inhibitory amino acid neurotransmitter in the mammalian central nervous system[33]. GABA modulates glutamic acid synaptic activity. Thus, abnormality of the GABAergic system can lead to a high neuronal excitability and reperfusion injury. In adult animals, GABA plays a protective role mainly through the activation of GABA receptors and increasing the flow of Cl⁻, resulting in the hyperpolarization of the postsynaptic membrane. Gabbr1 gene down-regulation is destined to affect nervous system signal transduction, and other normal functions

There is a negative regulator of the bone morphogenetic protein (BMP) signaling pathway, which leads to the down-regulation of the Wnt receptor signaling pathway Sostdc1 (FC = 0.31). BMP is a member of the transforming growth factor superfamily and plays an important role in skeletal development and bone morphogenetic formation. At the same time, BMP has a wide range of biological activities; it is a multifunctional protein involved in the morphogenesis of a variety of tissues and organs. Studies have shown that BMP signals are essential for neural development and its functions include the determination of the early neural ectoderm, distribution patterns and proliferation of the spinal cord, as well as embryonic and postnatal brain development[34-35]. Moreover, BMP binding with the BMP receptor signaling pathways has important cellular functions in the adult central nervous system. BMP is not only involved in the nervous system development process, but also participates in neurological diseases, such as injury repairing process[36-38].

Another down-regulated gene in the $A\beta_{1-40}$-induced AD model group, Atxn1 (Ataxin-1), is mainly located within the nucleus and serves to influence the cellular physiological and biochemical reactions through reaction with cell components within the nucleus. This response is enhanced in parallel with increasing CAG quantity. If Ataxin-1 is expressed in the cytoplasm, it is not pathogenic. Ataxin-1 expression in the cytoplasm is another mechanism underling AD occurrence. Atxn1 (Ataxin 1 protein) contributes to brain morphogenesis, adult motor behavior, visual learning, inhibition of transcription and RNA export from the nucleus, and regulation of postsynaptic membrane potential excitability[39-40].

Catechol-O-methyltransferase is ubiquitously present in the human body, and participates in catecholamine metabolism, neurotransmitter, dopamine, S-adenosyl homocysteine acid metabolism, and synthesis of biogenic amines. Catechol-O-methyltransferase is an

important biologically active substance affecting the functions of the brain. It can deactivate catechol biological activity, and its substrates are catechol hormones and neurotransmitters, such as epinephrine, norepinephrine, and dopamine. When the above-mentioned neurotransmitters are dysfunctional, they may induce nervous or mental diseases such as AD, Parkinson's disease, schizophrenia, or depression. The abnormal expression of catechol-O-methyltransferase gene is bound to affect the development and function of the nervous system, and thus, influences the occurrence and development of Parkinson's disease, AD, and other neurodegenerative diseases[41-44].

In this study, the Wnt receptor and BMP signal transduction pathway associated with nervous system development and function, and the Ras signaling pathway associated with cellular growth and differentiation, showed down-regulated expressions of several genes in the AD model group. The calcium and G protein-mediated signaling pathway, which contributes to the nervous system functions, also showed differentially expressed genes.

Based on the above findings, we conclude that the hippocampus of the AD model rats is under high stress, involving oxidative stress, inflammation *via* the immune response, cellular growth and differentiation, cellular cycle and apoptosis, energy metabolism, ion channel/transporter, cellular signal transduction, and other physiological and pathological processes. The effects of $A\beta_{1-40}$ on hippocampal gene expression are mainly achieved through the genes involving the immune and inflammatory response and cell signaling pathway genes involved in nervous system development and function, such as Wnt, Statin, Notch, Bmp, Ras, NF-κB, G protein receptor and Ca^{2+}. In addition, $A\beta_{1-40}$ can influence energy metabolism, and regulate cellular growth and apoptosis. This study aimed to elucidate the etiology and pathogenesis of AD in a broader attempt to provide gene targets for AD gene therapy.

MATERIALS AND METHODS

Design
A randomized, controlled, animal experiment.

Time and setting
Experiments were performed from February 2008 to February 2010 in the Central Laboratory at the First Affiliated Hospital of Shenzhen University (Shenzhen Second People's Hospital) and the Animal Laboratory in the Clinical Medicine College of Jinan University (Shenzhen People's Hospital), China.

Materials

Animals
Sprague-Dawley male rats, aged 6−8 weeks, weighing 200 ± 20 g, were purchased from the Experimental Animal Center of Guangdong Province, with license No. SCXK (Yue) 2008-0002 and Guangdong Monitoring and Certificate No. 2008A020. Prior to the experiment,

experimental rats were fed for 2 weeks, in a specific pathogen-free grade rearing environment, at 20−25°C, in relative humidity of 50 ± 5%, under a 12-hour day/night cycle. Experimental protocols were in strict accordance with the *Guidance Suggestions for the Care and Use of Laboratory Animals*, issued by the Ministry of Science and Technology of China[45].

Drugs
$A\beta_{1-40}$ (Sigma, St. Louis, MO, USA; 2 mg) dissolved in 1 mL normal saline after autoclaving was used to prepare a 2 μg/μL solution and incubated at 37°C constant temperature incubator for 7 days for the aging process, then stored at 4°C for further use.

Methods

Establishment of AD model animals with $A\beta_{1-40}$
In the AD model group, rats were weighed before surgery after 12-hour fasting and anesthetized *via* intraperitoneal injection of pentobarbital sodium (45 mg/kg) for 10 minutes. Rats were fixed in a stereotaxic instrument (RWD Life Science Co., Ltd., Shenzhen, China) and the head was surgically cut to expose the skull. According to the positions (anterioposterior −3.0 mm, mediolateral 2.0 mm) in the Rat Brain Stereotaxic Atlas[46], the rat skull was drilled at a diameter of 1.0−2.0 mm, and needles were slowly inserted (1 mm/min) into the bilateral hippocampi (dorsoventral 2.9 mm), while maintaining the integrity of the dura mater. AD animals were established through the injection of fore-processed condensed $A\beta_{1-40}$ (1 μL/min; supplementary Figure 1 online). Each rat was injected with $A\beta_{1-40}$ 50 ng/g; total volume in each injection was no more than 10 μL. After injection, the needle was retained for 5−10 minutes and slowly withdrawn (1 mm/min), followed by the suture of the scalp. Rats were postoperatively injected with penicillin 480 000 U/kg per day for 3 days and housed in separated cages. They were fasted for 12 hours post-surgery and received a regular diet on the next day (supplementary Figure 2 online). Sham-operated rats were injected with 10 μL sterile saline.

Behavioral test was performed using the Morris water maze (Panlab Co., Barcelona, Spain) at 4 weeks after the $A\beta_{1-40}$ injection, to observe and compare the decline of learning and memory abilities in the animals, and to screen out the successful AD model rats. The test included space navigation and space probe sections. Escape latency, swimming time and distance, and search time were recorded. The time and route to each quadrant were automatically analyzed with water maze software, then the percentage of the time and route of rats swimming in the original platform quadrant to the total duration and searching distance was calculated[47]. The average escape latency of each rat was calculated to screen out eight qualified rats, according to the determination criteria that takes +2 times of the standard deviation of the mean escape latency of normal controlled rats as the lower limit, while +1 time of the standard deviation of their mean escape latency was the maximum. The hippocampal tissues were randomly

harvested from five of the eight rats.

Total RNA extraction from rat hippocampus

Five rats in each group were randomly selected. The brains were conventionally harvested under sterile condition (supplementary Figure 3 online). The surface fascia tissue was removed after washing with PBS and bilateral hippocampal tissue was carefully isolated (supplementary Figure 4 online). The specimens were immediately transferred to cryopreservation tubes or wrapped in aluminum foil in gauze bags, and stored in liquid nitrogen for further use.

Before the extraction of RNA, the tissues were ground for 8–10 minutes in a mortar that had been pre-cooled with liquid nitrogen, and liquid nitrogen was repeatedly added to avoid evaporation to dryness. The amount of the tissue for grinding was no more than 300 mg. The ground tissue powder was mixed with 2.0–3.0 mL Trizol reagent (Invitrogen Life Technologies, Carlsbad, CA, USA) and Trizol reagent was then transferred to 1.5-mL centrifugation tubes. Total RNA was extracted according to the standard use of Trizol reagent[48]. Tissues were centrifuged at 12 000 r/min for 5 minutes, and the precipitates were discarded. Specimens were mixed with 200 μL chloroform and placed on ice for 15 minutes, and centrifuged at 4°C, at 12 000 r/min for 15 minutes. The upper aqueous phase was collected and transferred to another centrifuge tube, mixed with equal volume of pre-cooled isopropanol and stored at −20°C for more than 2 hours or overnight. Specimens were centrifuged at 4°C, 12 000 r/min for 10 minutes and the supernatant was discarded. Specimens were mixed with 1 mL 70–80% ethanol and the centrifuge tube was moderately oscillated until the precipitates were suspended. Specimens were again centrifuged at 4°C, 8 000 r/min for 5 minutes, and the supernatant was discarded. RNA precipitating at the bottom of tube was dried at room temperature or under vacuum for 5–10 minutes. The harvested RNA was dissolved in 20–30 μL DEPC-treated deionized water.

The concentration and purity of 2–5 μL RNA was detected with a UV-visible spectrophotometer (U-3310, Hitachi, Tokyo, Japan), and its integrity was assayed with formaldehyde denaturing gel electrophoresis[49]. Total RNA (0.3 μg) was mixed with 1/5 volume of 5 × loading buffer, and was heated to 65°C for 5 minutes, and then quenched on ice to remove the RNA secondary structures. RNA samples before the sampling were treated with 0.5–1.0 μL of ethidium bromide (1.0 mg/mL). Formaldehyde denaturing gel (1.2%) was placed in 1 × formaldehyde denaturing gel electrophoresis buffer for 15 minutes. RNA samples were subjected to electrophoresis for 30 minutes at 5–10 V/cm voltage.

Microarray analysis

Gene microarray analysis was performed in the CapitalBio Corporation (the National Engineering Research Center for Beijing Biochip Technology, China). The target samples were prepared with a single-cycle cRNA amplification and biotin labeling method for microarray hybridization. Samples were eluted and stained with Fluidics Station 450 (Affymetrix, Santa Clara, CA, USA), and the chip was scanned with Affymetrix GeneChip Scanner 3000 (Affymetrix), and images were analyzed with Affymetrix GeneChip Operating Software Version 1.4 software. The image signal was transformed into digital signals, then the images were corrected and normalized with dChip software (Cheng Li Lab, Harvard University, Cambridge, MA, USA). The fluorescence signal intensity and ratio were analyzed with SAM 2.10 (Significance analysis of microarrays 2.10, written by Balasubramanian Narasimhan and Robert Tibshirani, Stanford University, Stanford, USA). Finally, the differentially expressed genes were screened out according to the criteria of two-fold differences (q value (%) < 1 %, FC ≥ 2 or ≤ 0.5)[50]. The cluster analysis of the signal value of each sample was performed with cluster3.0 (written by Michael Eisen, Stanford University, Palo Alto, CA, USA; updated in 2002 by Michiel de Hoon, University of Tokyo, Tokyo, Japan), and calculated with a hierarchical, average linkage algorithm. The function and signal transduction pathway of differentially expressed genes were determined with MAS (CapitalBio Molecule Annotation System V 4.0, CapitalBio Corporation/the National Engineering Research Center for Beijing Biochip Technology, China).

REFERENCES

[1] Masliah E. Neuropathology: Alzheimer's in real time. Nature. 2008; 451(7179):638-639.
[2] Small DH. Network dysfunction in Alzheimer's disease: does synaptic scaling drive disease progression? Trends Mol Med. 2008;14(3):103-108.

[3] Li M, Chen L, Lee DH, et al. The role of intracellular amyloid beta in Alzheimer's disease. Prog Neurobiol. 2007;83(3):131-139.

[4] Moreno H, Wu WE, Lee T, et al. Imaging the Abeta-related neurotoxicity of Alzheimer disease. Arch Neurol. 2007;64(10): 1467-1477.

[5] Mruthinti S, Capito N, Sood A, et al. Cytotoxicity of Abeta1-42, RAGE23-54, and an Abeta-RAGE complex in PC-12 cells. Curr Alzheimer Res. 2007;4(5):581-586.

[6] Irie K, Murakami K, Masuda Y, et al. The toxic conformation of the 42-residue amyloid beta peptide and its relevance to oxidative stress in Alzheimer's disease. Mini Rev Med Chem. 2007;7(10): 1001-1008.

[7] Jain KK. Tech.Sight. Biochips for gene spotting. Science. 2001; 294(5542):621-623.

[8] Orlov YL, Zhou J, Lipovich L, et al. Quality assessment of the Affymetrix U133A&B probesets by target sequence mapping and expression data analysis. In Silico Biol. 2007;7(3):241-260.

[9] Roxas BA, Li Q. Significance analysis of microarray for relative quantitation of LC/MS data in proteomics. BMC Bioinformatics. 2008;9:187.

[10] Grewal A, Lambert P, Stockton J. Analysis of expression data: an overview. Curr Protoc Bioinformatics. 2007;Chapter 7:Unit 7.1.

[11] Kaba B, Pinet N, Lelandais G, et al. Clustering gene expression data using graph separators. In Silico Biol. 2007;7(4-5):433-452.

[12] Lee YS, Tsai CN, Tsai CL, et al. Comparison of whole genome amplification methods for further quantitative analysis with microarray-based comparative genomic hybridization. Taiwan J Obstet Gynecol. 2008;47(1):32-41.

[13] Holtz WA, Turetzky JM, O'Malley KL. Microarray expression profiling identifies early signaling transcripts associated with 6-OHDA-induced dopaminergic cell death. Antioxid Redox Signal. 2005;7(5-6):639-648.

[14] Lien WH, Klezovitch O, Fernandez TE, et al. AlphaE-catenin controls cerebral cortical size by regulating the hedgehog signaling pathway. Science. 2006;311(5767):1609-1612.

[15] Ridley RM, Baker HF, Leow-Dyke A, et al. Further analysis of the effects of immunotoxic lesions of the basal nucleus of Meynert reveals substantial impairment on visual discrimination learning in monkeys. Brain Res Bull. 2005;65(5):433-442.

[16] Su BG, Xu LX. Morphological observation of synaptic plasticity of hippocampal formation induced by activity of spatial learning and memory. Jiepou Xue Zazhi. 2003;26(1):25-39.

[17] Chu J, Li L. The dementia models induced by intracerebroventricular infusion of β-amyloid peptide in mice. Zhongguo Yaoli Xue Tongbao. 2004;20(7):827-829.

[18] Ehebauer M, Hayward P, Martinez-Arias A. Notch signaling pathway. Sci STKE. 2006;2006(364):cm7.

[19] Louvi A, Artavanis-Tsakonas S. Notch signalling in vertebrate neural development. Nat Rev Neurosci. 2006;7(2):93-102.

[20] Artavanis-Tsakonas S, Rand MD, Lake RJ. Notch signaling: cell fate control and signal integration in development. Science. 1999; 284(5415):770-776.

[21] Gaiano N, Fishell G. The role of notch in promoting glial and neural stem cell fates. Annu Rev Neurosci. 2002;25:471-490.

[22] Fan X, Mikolaenko I, Elhassan I, et al. Notch1 and notch2 have opposite effects on embryonal brain tumor growth. Cancer Res. 2004;64(21):7787-7793.

[23] Zheng YF, Zheng ZX. Notch signaling in the neural tumorigenesis. Zhonghua Zhongliu Fangzhi Zazhi. 2007;14(13):1029-1032.

[24] Hu YA, Zhao CJ. Research progress of Wif1 in development of nervous system. Zhejiang Da Xue Xue Bao Yi Xue Ban. 2010; 39(1):93-96.

[25] Cai LY, Zhao B, Wang SK. Wnt signaling pathway and spinal cord injury. Guoji Guke Xue Zazhi. 2010;31(2):119-120,127.

[26] Han PP, Zheng RN. Wnt signal pathway and its role in disease. Shengwu Jishu Tongbao. 2009(11):13-15.

[27] Li YF, Guan YJ, Yu L. Progress in research of relationship between Wnt signaling pathway and neural tube defects. Shenjing Jiepou Xue Zazhi. 2009;25(2):236-238.

[28] Hong DJ, Zhu CQ. Presenilin interacts with Notch and Wnt signal pathway in Alzheimer's disease. Shengming de Huaxue. 2002; 22(1):47-49.

[29] Zhang X, Li Y. Research progress in the role of Wnt signaling pathway in Alzheimer's disease. Zhonghua Shenjing Yixue Zazhi. 2008;7(4):430-432.

[30] Delanty N, Vaughan CJ, Sheehy N. Statins and neuroprotection. Expert Opin Investig Drugs. 2001;10(10):1847-1853.

[31] Cucchiara B, Kasner SE. Use of statins in CNS disorders. J Neurol Sci. 2001;187(1-2):81-89.

[32] Zacco A, Togo J, Spence K, et al. 3-hydroxy-3-methylglutaryl coenzyme A reductase inhibitors protect cortical neurons from excitotoxicity. J Neurosci. 2003;23(35):11104-11111.

[33] Frahm C, Haupt C, Witte OW. GABA neurons survive focal ischemic injury. Neuroscience. 2004;127(2):341-346.

[34] Wang YP, Jiang XH, Zuo DQ, et al. BMP signal and its role in central nervous system. Guoji Jingshenbing Xue Zazhi. 2008; 35(1):27-29.

[35] Liu A, Niswander LA. Bone morphogenetic protein signalling and vertebrate nervous system development. Nat Rev Neurosci. 2005; 6(12):945-954.

[36] Hall AK, Miller RH. Emerging roles for bone morphogenetic proteins in central nervous system glial biology. J Neurosci Res. 2004;76(1):1-8.

[37] See J, Zhang X, Eraydin N, et al. Oligodendrocyte maturation is inhibited by bone morphogenetic protein. Mol Cell Neurosci. 2004; 26(4):481-492.

[38] Grinspan JB, Edell E, Carpio DF, et al. Stage-specific effects of bone morphogenetic proteins on the oligodendrocyte lineage. J Neurobiol. 2000;43(1):1-17.

[39] Banfi S, Servadio A, Chung M, et al. Cloning and developmental expression analysis of the murine homolog of the spinocerebellar ataxia type 1 gene (Sca1). Hum Mol Genet. 1996;5(1):33-40.

[40] Tong X, Gui H, Jin F, et al. Ataxin-1 and Brother of ataxin-1 are components of the Notch signalling pathway. EMBO Rep. 2011; 12(5):428-435.

[41] Nissinen E, Männistö PT. Biochemistry and pharmacology of catechol-O-methyltransferase inhibitors. Int Rev Neurobiol. 2010; 95:73-118.

[42] Meeks TW, Ropacki SA, Jeste DV. The neurobiology of neuropsychiatric syndromes in dementia. Curr Opin Psychiatry. 2006;19(6):581-586.

[43] Di Giovanni S, Eleuteri S, Paleologou KE, et al. Entacapone and tolcapone, two catechol O-methyltransferase inhibitors, block fibril formation of alpha-synuclein and beta-amyloid and protect against amyloid-induced toxicity. J Biol Chem. 2010;285(20): 14941-14954.

[44] Forero DA, Benítez B, Arboleda G, et al. Analysis of functional polymorphisms in three synaptic plasticity-related genes (BDNF, COMT AND UCHL1) in Alzheimer's disease in Colombia. Neurosci Res. 2006;55(3):334-341.

[45] The Ministry of Science and Technology of the People's Republic of China. Guidance Suggestions for the Care and Use of Laboratory Animals. 2006-09-30.

[46] Bao XM, Shu SY. The Rat Brain in Stereotaxic Coordinates. Beijing: People's Medcial Press. 1991.

[47] Lesné S, Koh MT, Kotilinek L, et al. A specific amyloid-beta protein assembly in the brain impairs memory. Nature. 2006;440(7082): 352-357.

[48] Ovstebø R, Olstad OK, Brusletto B, et al. Identification of genes particularly sensitive to lipopolysaccharide (LPS) in human monocytes induced by wild-type versus LPS-deficient Neisseria meningitidis strains. Infect Immun. 2008;76(6):2685-2695.

[49] Sambrook J, Russel DW. Molecular Cloning. A Laboratory Manual. Cold Spring Harbor: Cold Spring Harbor Laboratory. 2001.

[50] Tusher VG, Tibshirani R, Chu G. Significance analysis of microarrays applied to the ionizing radiation response. Proc Natl Acad Sci U S A. 2001;98(9):5116-5121.

(Edited by Cao P, Li R/Yang Y/Song LP)